

Characterization of Instabilities in a Low-Swirl Injector with Exhaust Gas Recirculation

Don Ferguson¹ and Joseph Ranalli²

National Energy Technology Laboratory, Morgantown, WV 26507

There is an international effort to reduce greenhouse gases, including carbon dioxide emissions. In terms of addressing CO₂ emission from power plants, post-combustion carbon capture is viewed as a near term solution, as it does not require redesign of the entire plant. Various post-combustion carbon absorption strategies are available. In implementing this type of device, Exhaust Gas Recirculation has been proposed, because it offers cost reduction benefits for absorption hardware by reducing the total flow rate that needs to be processed, and by increasing the concentration of CO₂ in the exhaust gas. However, EGR represents a change in the reactant gases, for which the effect on the combustion process needs to be understood.

Changes in fuel composition may be especially have an impact on flame dynamics. Tests will be performed in a lean-premixed combustor with High and Low Swirl Injectors. Methane and Methane/Hydrogen blends will be tested with EGR simulated by dilution with nitrogen and carbon dioxide. Instabilities will be characterized by the velocity oscillation amplitude and frequency, to draw conclusions about the impact EGR has on combustor operation.

I. Introduction

Post-combustion carbon capture utilizing an amine-based¹ or solid² absorbent is a currently viable technology that could be used to reduce greenhouse gases emissions from stationary power generation applications. As a retrofit to existing plants, post-combustion carbon capture addresses the immediate, short-term need while advanced technologies such as integrated gasification combined cycle (IGCC) or integrated gasification fuel cell (IGFC)² continue to develop. However, as recent estimates suggest that adding a carbon capture system to an existing plant could add as much as 30% to the cost of electricity³ and impact the overall plant efficiency, without significant regulatory or economic changes it is unlikely to gain support. The bulk of the cost is related to the relative size of the system that most considered. Exhaust gas from a natural gas fired gas turbine may contain approximately 4-14% CO₂, however, post-combustion carbon capture systems must be sized to accommodate the total exhaust flow requiring large and expensive equipment.

Exhaust gas recirculation (EGR) offers a strategy for concentrating the CO₂ content in the flue gas while at the same time reducing the total volume of flow that must pass through a post-combustion carbon capture system. El Kady et al.⁴ demonstrated operation of an F-class scale combustor utilizing a lean premixed fuel injection with up to 35% EGR. In addition to increasing the CO₂ content in the exhaust stream without adversely impacting the CO emissions, the authors also saw a 50% reduction in NO_x emissions. Similar results were obtained by Rokke et al.⁵ and Li et al.⁶. However the effect of EGR on gas turbine combustion must be understood before the technology is mature enough for utilization in the field. In particular concerns over lean blow-out (LBO) and thermoacoustic instabilities must be addressed.

Conventional gas turbine combustors may utilize lean premixed (LPM) combustion to achieved low NO_x emissions. These systems typically utilize a swirl-stabilized fuel injection system to pre-mix the fuel and anchor the flame in the combustor. The extent of swirl and anchoring mechanism can have a direct impact on flame stability particularly when varying the fuel composition through fuel dilution such as EGR.

¹ Research Engineer, Member AIAA, donald.ferguson@netl.doe.gov

² Postdoctoral Research Associate, Member AIAA, joseph.ranalli@or.netl.doe.gov

The study presented in this work focuses on the influence of simulated EGR on dynamic combustion (thermoacoustic) instabilities in swirl-stabilized flames with methane and methane/hydrogen blended fuels. Tests are performed on a lab-scale, swirl-stabilized, atmospheric burner with both a conventional high-swirl (HSI) and a novel low-swirl injector (LSI). EGR is simulated by the addition of 0-10% CO₂ and 0-20% N₂. Fuel compositions and operating conditions were pre-determined to ensure test cases with overlapping flame temperatures as previous researchers have found strong correlation between thermoacoustic instabilities and flame temperature in lean-premixed combustion. Under conditions of self-excited instability the convective time delay of acoustic velocity perturbations and flame interaction were determined and related to changes in the flame shape as a result of EGR and changes in swirl number.

II. Background

In order to achieve the required limitation on pollutant emissions, gas turbine manufacturers rely on lean premixed (LPM) to help reduce peak flame temperatures and subsequently lower NO_x emissions. However, the loss of downstream dilution and changes in combustor geometries associated with LPM has led to a greater occurrence of dynamic combustion, or thermoacoustic, instabilities. Thermoacoustic instabilities are the result of closed-loop coupling between the combustor system acoustics and unsteady heat release. A periodic disturbance that originates within the reactants is convected to the flame where it, after a short chemical time, produces a periodic variation in the heat release.

From the description of this coupling mechanism it is apparent that flame location, flame shape and fuel composition play a critical role. Lieuwen and Zinn⁷ discussed how small changes in the fuel-air mixture could produce significant changes in the convective time delay and subsequently heat release oscillations for lean-premixed flames. A number of other studies have considered the influence of fuel composition on combustion instabilities^{8,9,10,11,12,13}. Wicksall and Agrawal¹⁰ investigated the influence of hydrogen augmentation on methane flames with results indicating an increase in the total sound power with an increase in the adiabatic flame temperature. A similar study performed by Tuncer et al.¹⁴ considered the dynamic response of a hydrogen-enriched methane flame giving anecdotal evidence of a change in the flame center of mass as a result of an increase in flame speed. Unfortunately supportive quantitative results were not provided. Hendricks and Vandsburger¹¹ measured the Frequency Response Function of various hydrocarbon flames exposed to open-loop forcing of the flame and showed that varying the fuel content could drive or damp the instability depending on the mode of the instability. Chemical kinetic studies, not specifically directed towards thermoacoustic instabilities, such as Cong and Dagaut¹⁵ and Liu et al.¹⁶ have shown that although the primary influence of CO₂ is through a thermal effect, there is a secondary chemical effect as a result of the reaction $\text{CO} + \text{OH} \leftrightarrow \text{CO}_2 + \text{H}$ that produces a decrease in the rate of fuel consumption. In terms of combustion instabilities this could alter the heat release distribution or the convective time delay and could impact the dynamic response as described below.

Disturbances originating in the nozzle are convected to the flame where they produce a perturbation in the combustion heat release which in turn drives the instability⁷. Richards et al.¹² discussed this time-delay model and argued that in order for closed-loop dynamics to occur the time delay must be a function of the acoustic period $T = 1/f$, where “f” is the frequency, thus $\tau = kT$ which is dependent on the acoustic characteristics of the combustion chamber. The convective time delay can be expressed as a relationship between the sum of convective and chemical time scale⁸:

$$\tau_{\text{conv}} + \tau_{\text{chem}} = kT \quad (1)$$

where τ_{conv} represents the time required for a disturbance to propagate from its point of origin to the flame “center of mass”, and τ_{chem} is the chemical time that elapses as a result of combustion at the flame center of mass. A convenient way to describe the flame dynamics is in terms of Strouhal number (non-dimensional frequency) based on these convective phenomena. The Strouhal number may be thought of as the ratio between the time taken for a disturbance to convect along a characteristic length x_c , at a mean convective velocity u_c , and the period of oscillation $1/f$ and is defined as follows:

$$St = \frac{f \cdot x_c}{u_c} \quad (2)$$

The characteristic length is often based on the distance from the dump plane to the location of the flame center-of-mass, or the total flame length measured from the dump plane¹⁷.

The flame anchoring mechanism, as previously noted, plays a key role in defining the convective time delay and the flame stability. In conventional LPM systems a swirling flow enters the combustion chamber and creates a low pressure zone in the wake of a centerbody at the exit of the nozzle. A central, or inner, recirculation zone (IRZ) forms and along with accompanying outer recirculation zones (ORZ) recirculates hot combustion products resulting in sustained combustion. The size and intensity of the IRZ is defined primarily by the rate of rotation of the swirl which is characterized by the ratio of tangential to axial momentum flux, or swirl number¹⁸.

$$S = \frac{\int_0^R \rho u v 2\pi r^2 dr}{R \int_0^R \rho u^2 2\pi r dr} \quad (3)$$

Where ρ is the fluid density, u and v the axial and azimuthal velocity, respectively, r the radius and R the characteristic outer radius. Typical industrial gas turbines operate with a swirl number ranging from $0.6 < S < 1.6$ ¹⁹. Changes in the swirl number can have a direct impact on the flame shape and in particular on the flame spreading angle as defined by the angle of the flame from the axial centerline. This will in turn effect the convective time as the distance changes between the nozzle exit and flame center of mass.

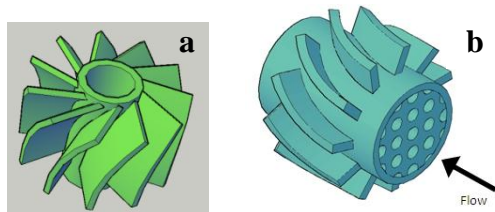


Figure 1a and b. CAD drawing of the high and low-swirl injectors used in this study. The arrow on the LSI indicates the flow direction.

Changes in the flame angle and heat release distribution may also produce a local change in the coupling between the velocity and heat release perturbations, or flame transfer function (FTF). Kim et al.²⁰ considered the spatial distribution flame transfer functions in swirl stabilized flames. They found that changes in the flame length [as a result of changes in operating conditions or fuel composition] altered the predictive capability of the FTF and once a flame length reached a critical length, local FTFs were found to provide a better prediction of phase/gain coupling than the respective global FTF. Palies et al.¹⁸ also considered spatially distributed transfer functions by splitting phase resolved images of an acoustically forced flame into an upper and lower region. Their analysis showed that at some frequencies the upper and lower regions produced constructive interference resulting in higher gain, while at other frequencies destructive interference resulting in damping.

Unlike conventional injectors that utilize high swirl ($S > 0.6$), low swirl injectors support an aerodynamically stabilized flame. The LSI consists of two passages: an outer annulus with swirl vanes and an open center channel (Figure 1). The center channel is fitted with a perforated plate to control the flow split between the inner and outer channels. As this is an aerodynamically stabilized flame, it relies on the flame propagation speed and the rate of flow divergence defined by the flow split to control the flame lift off distance. An interesting characteristic of the LSI is stability of the flame lift off distance given $U_o \gg S_L$, where U_o is the bulk flow velocity and S_L is the laminar flame speed²¹.

Few studies have attempted to characterize the flame dynamics for a flame stabilized using a low-swirl injector. Kang *et al.*²² made measurements of the spatially resolved Rayleigh Index, a quantity describing essentially the phasing of the thermoacoustic coupling, in forced flames and found a relationship between instabilities and toroidal structures in the shear mixing region near the flame boundary. Yilnaz et al.²³ found similar results in the Rayleigh Index distribution including the effects of hydrogen addition.

III. Experimental Methodology

The combustor used in this study is an atmospheric pressure laboratory-scale dump combustor similar to that used previously by the authors²⁴ and shown in Figure 2, with the exception that both low- and high-swirl injection are being considered. As the fuel and air are premixed well upstream of the combustor, the “injectors” are merely a set of swirl vanes positioned 38 mm and 29.5 mm upstream of the dump plane for the high and low swirl injectors, respectively. The high swirl vane configuration (geometric swirl number of ~ 0.88) is shown in Figure 1a include a centerbody that extends axial through the center of the swirl vane to the dumplane of the combustor. This arrangement, as described above, creates a low pressure field at the nozzle exit resulting in the flame anchoring on the outer radius of the centerbody. Alternately, the low swirl vane geometry (geometric swirl number ~ 0.5)

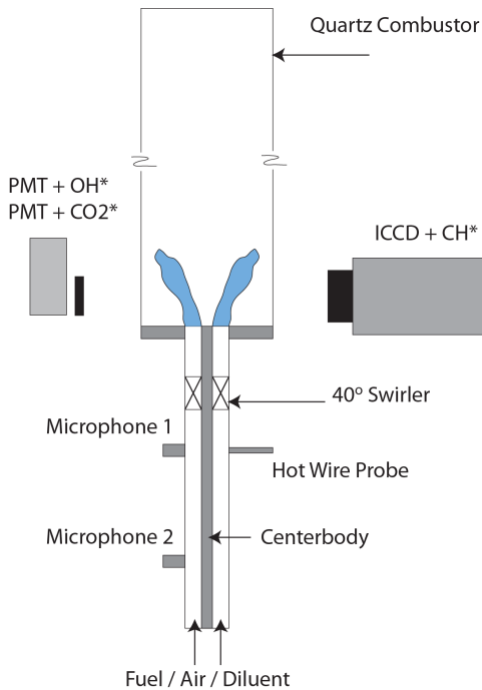


Figure 2 - Experimental apparatus showing HSI configuration.

Case A consisted of pure methane as a baseline, with cases B through D showing the effects of nitrogen or carbon dioxide dilution. Cases E and F represent test conditions in which both hydrogen addition to the fuel, and nitrogen or carbon dioxide dilution are present. Fuel-diluent combinations were selected in order to overlap the flame temperature in regions prone to instabilities for the baseline fuel. Reported flame temperatures were calculated at equilibrium using Cantera and GRI-Mech 3.0 chemistry.

Spatially resolved chemiluminescence was recorded using an intensified camera narrow band filtered at 431 nm for CH* emission with a resolution of 94 μm per pixel. These images were acquired with an intensifier gate of 5ms, approximately integrating over one full cycle of the unstable operation (around 200Hz). Ten such images were averaged at each operating condition to reduce the impact of transient behavior, Fig 3a and c. Each average image

was deconvoluted assuming axial symmetry using an Abel Transform (Fig 3b and d). The upstream and downstream flame edges were identified by thresholding of the steady CH* chemiluminescence images using levels determined algorithmically by the MATLAB Image Processing Toolbox GRAYTHRESH routine.

Nondimensionalization of the frequency via the Strouhal number requires a characteristic length and velocity. The velocity was calculated using the mean nozzle velocity based on the flow

rate and area of the nozzle tube (21.6 mm diameter). It should be noted that given the difference in the flow distributions for each swirl configuration this approximate nozzle velocity does not necessarily indicate the exact local convective velocity. However, it is assumed that the approximated velocity should maintain a proportional relationship with the actual convective velocity.

produces an aerodynamically stabilized flame through a balance between the central, axial flow and the rotating exterior flow allowing the flame to anchor in the shear region.

The injector is mounted in a 21.6 mm diameter nozzle which rapidly expands into a 79mm diameter quartz combustion section. A “long” (0.56 m) quartz tube was used to provide sufficient acoustic gain for the combustor to become self-excited. The mean and perturbation velocities were measured directly upstream of the swirler using a hotwire anemometer inserted through a port in the nozzle. The flame heat release rate was characterized using a global measurement of the OH* radical chemiluminescence²⁵. The OH* chemiluminescence measurement was made using a Photomultiplier Tube (PMT) filtered at the 308nm OH* emission.

Fuel, air and diluent were metered using a set of mass flow controllers. Mixing occurred upstream of a choke plate mounted in the base of the nozzle in order to acoustically decouple the mixing section from the rest of the combustor, preventing the occurrence of equivalence ratio or diluent concentration oscillations. A variety of fuel / diluents combinations were evaluated (Table 1), including CH4 and H2 fuel blends with varying levels of CO2 and N2 dilution to simulate EGR. Dilution levels are reported as a percentage of the total volumetric flow rate and in the case of N2 dilution, the stated dilution percentage represents only the additional N2 added to the flow and excludes the amount of nitrogen already present with the reactant air flow.

Table 1 – Test Matrix

	A	B	C	D	E	F
Phi	0.65-1.10	0.80-1.10	0.75-1.10	0.85-1.10	0.80-1.10	0.75-1.10
Total Flow (LPM)	100-150	100-150	100-125	100-150	100-150	100-140
Diluent Comp.						
CO2 (% Total)	0	10	0	0	10	0
N2 (% Total)	0	0	10	20	0	20
Fuel Composition						
CH4 (% Fuel)	100	100	100	100	75	75
H2 (% Fuel)	0	0	0	0	25	25
T adiabatic (K)	1754-2232	1790-2024	1790-2107	1790-1967	1802-2033	1663-1977

For this study the characteristic length is approximated as the distance the perturbation travels from the combustor dump plane to the flame center of mass. The center of mass was defined as the phase averaged center of the CH^* intensity (heat release rate) as recorded by the ICCD. For the high swirl, V-shaped flame the distance was characterized using the axial and radial distances to the flame center-of-mass, measured from the dump plane and the outer edge of the center-body where the flame was anchored (Figure 4a). These measurements are reported as a vector quantity, with a magnitude indicating the distance from the center-body tip and an angle representing the flame orientation relative to the vertical. In the case of the aerodynamically stabilized, low swirl injector a convenient location in which to define a vector quantity was not readily available thus the axial distance from the dump plane to the measured center of mass was used (figure 4b).

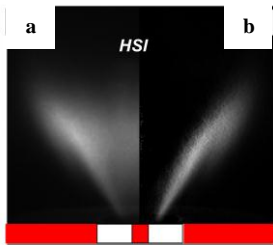


Figure 3a) Time-averaged image of unstable flame at $Q = 150$ lpm, $f = 0.95$, $V_{rms} = 0.3$; **3b)** Abel inverted image of the flame

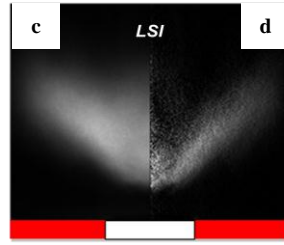


Figure 3c) Time-averaged image of unstable flame at $Q = 100$ lpm, $f = 0.80$, $V_{rms} = 0.02$; **3d)** Abel inverted image of the flame

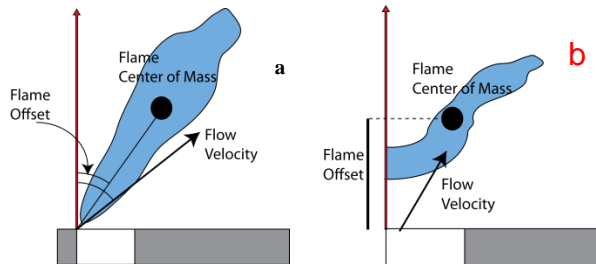


Figure 4- Schematic representation of flame “center of mass” in relation to burner geometry and flow direction for HIS (a) and LSI(b).

dynamic response for the CO_2 diluted fuel, but only had a small impact on the 20% N_2 diluted fuel.

The LSI combustor exhibited a slightly different behavior that trended closely with flame temperature regardless of fuel composition, Figure 5b. This is most likely the result of an aerodynamically stabilized flame that is less sensitive to changes in flame speed²¹ and with a flow field that is composed of both axial and azimuthal flow. Further tests are planned to evaluate the spatial flame transfer function distribution similar to other studies of high swirl stabilized combustion^{18,20} in order to validate the impact of the varying flow field. At temperatures greater than $T_{eq} = 2100$ K the peak response was twice that observed in the HSI, however it should be noted that at this condition the flame had propagated upstream to anchor in the fuel nozzle.

Figure 6a and 6b provides a qualitative comparison of the flame shape under periods of peak instability for both the HSI and LSI, respectively. Time average images suggest a change in flame shape with dilution that results in a subsequent change in the dynamic response. The observed behavior is similar to the results reported by Kim et al.²⁰ in which “V” shaped flames similar to flames with fuels A, C and E were more susceptible to flow disturbances than are enveloped “M” flames (Fuels B, D and F) as the later had less contribution of its flame tip to fluctuations. Additionally, these “V” shaped flames are more compact than the “M” and interference as a result of perturbations along the flame surface are more likely to be in phase or constructive.

IV. Results & Discussion

The dynamic response of the flame is shown as a function of flame temperature for flows of 125 lpm for both the HSI and LSI in Figure 5a-b. Responses from flows at 100 and 150 lpm were similar for both configurations thus only results from the 125 lpm case are shown here. While the response varies as a function of swirl, each plot shows a distinct change in the dynamic response once some threshold temperature is reached with the peak response occurring with the baseline fuel (A). However, while the low swirl response tends to agree with the results of Wicksall and Agrawal¹⁰ that displayed a strong dependency of dynamic amplitude on the flame temperature independent of fuel composition, the results from the high swirl configuration shown here suggest that at constant flame temperatures it is possible to modify the dynamic response through the addition of CO_2 or N_2 in both CH_4 and H_2/CH_4 flames.

The results from the HSI configuration shown in Figure 5a show a significant difference in dynamic response between flames with 10% CO_2 dilution (Fuel B) compared to those with 10% N_2 dilution (Fuel C) although the calculated equilibrium flame temperature is maintained. These results would suggest that flames diluted with 20% N_2 (Fuel D) had a response more similar to that of the 10% CO_2 diluted (Fuel B) case. The addition of 25% H_2 resulted in an increase in the

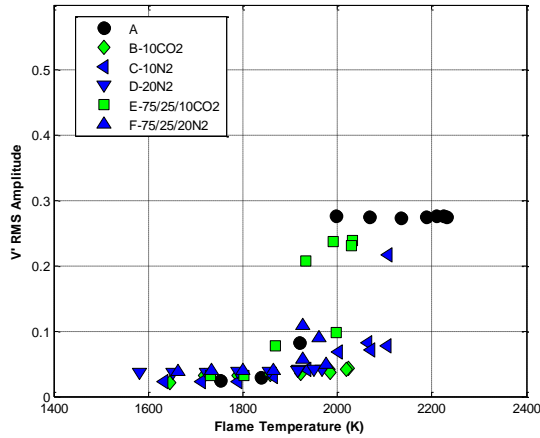


Figure 5a. Velocity perturbation RMS versus adiabatic flame temperature for $Q = 125$ lpm (HSI).

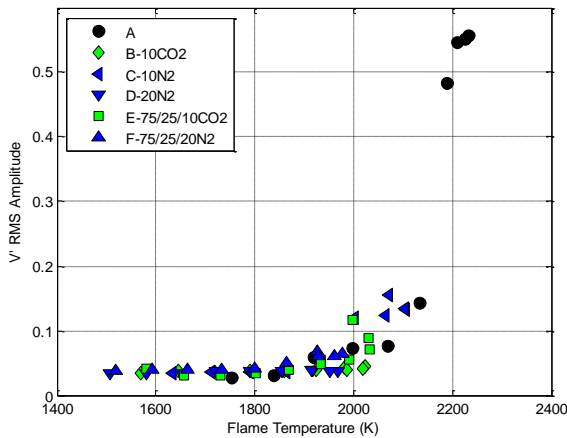


Figure 5b. Velocity perturbation RMS versus adiabatic flame temperature for $Q = 125$ lpm (LSI).

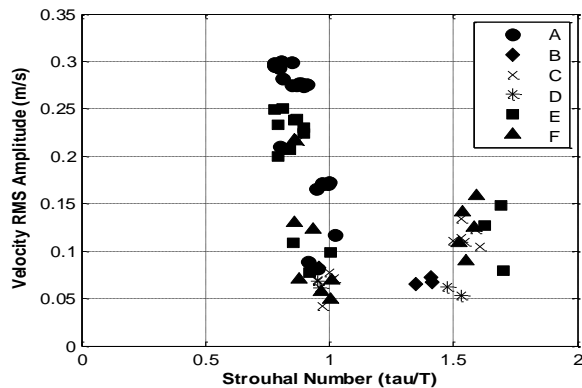


Figure 7a. Velocity perturbation amplitude plotted as a function of the non-dimensional time delay, Flame Strouhal Number (HSI).

Respective images from the LSI are somewhat different (Figure 6b) and support the insensitive nature of the flame to changes in fuel composition. Aside from the image of the peak response from Fuel A in which the flame has propagated upstream into the nozzle, only Fuel D and to a lesser degree Fuel B result in much change in the qualitative appearance of the flame.

Further investigation of the unstable behavior can be obtained from the non-dimensional frequency in terms of Strouhal number (Equation 2). By generating such a plot, we may see a slight bifurcation in the response for the HSI, Figure 7a, due to one additional period of delay later than the lower frequency mode. This effect has been described in the literature^{7,8} and is similar to the response obtained by Richards et al.¹²

As previously noted, the LSI configuration did not exhibit as strong a response to changes in fuel composition (Figure 7b). It should be noted that the selection of the actual distance used to describe the characteristic length may alter the absolute value of the Strouhal number thus making a comparison between the HSI and LSI somewhat difficult, however the general trend is similar. These results support the hypothesis that regions of the flame may be in and out of phase contributing to constructive/destructive interference and that the ratio between the convective time delay and acoustic period is a strong indicator of the potential for instability, although the gain must be greater than the damping for the system to be unstable.

The effect of EGR is best described through its effect on the time delay. In a practical turbine system, design reasons may lead us to fix the flame temperature. In the case of the HSI, at a fixed flame temperature the EGR cases were observed to result in increased time delay thus

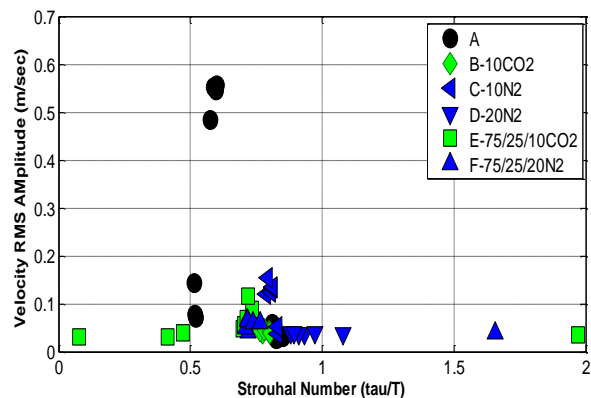


Figure 7b. Velocity perturbation amplitude plotted as a function of the non-dimensional time delay, Flame Strouhal Number (LSI).

High Swirl Combustion
Peak Instability Amplitude

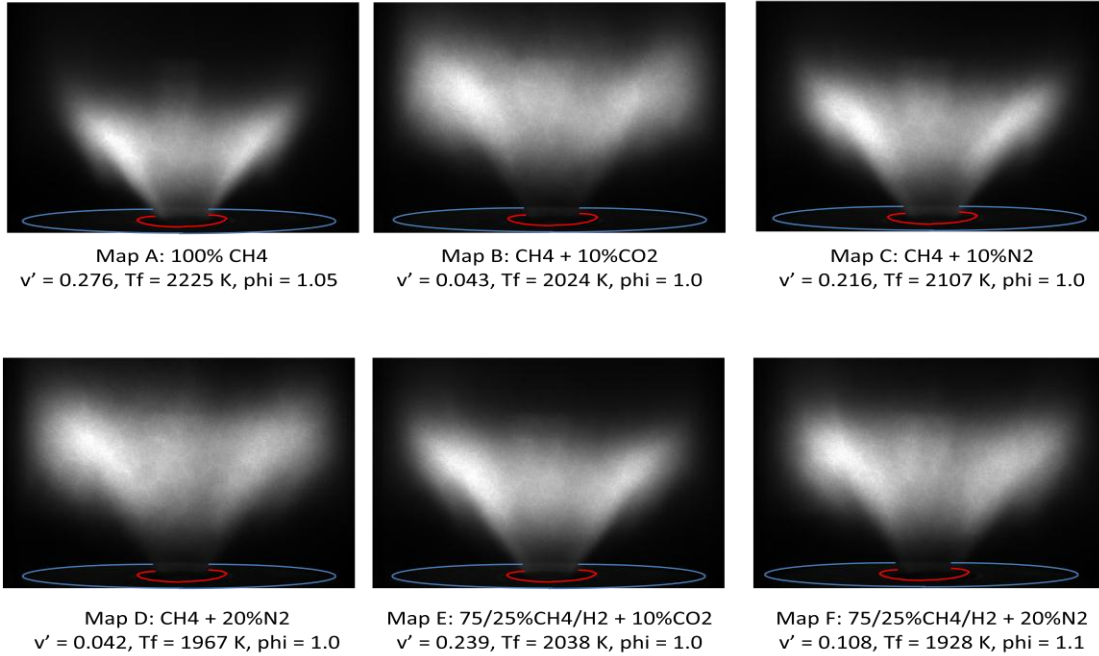


Figure 6a: Time solved images of the flame under conditions of peak instability (HSI)

Low Swirl Combustion
Peak Instability Amplitude

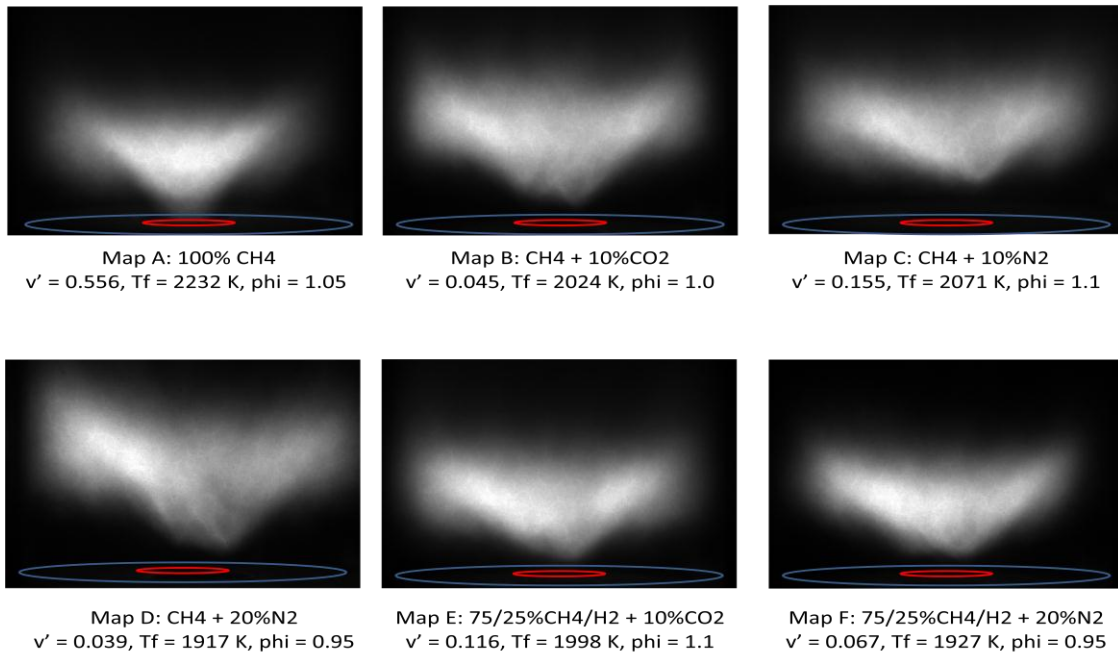


Figure 6b: Time solved images of the flame under conditions of peak instability (LSI)

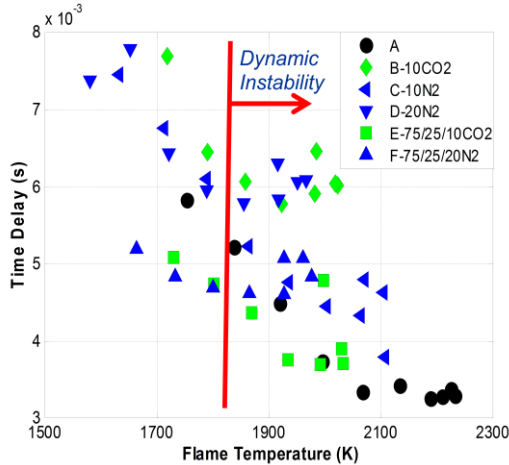


Figure 8a. The addition of fuel diluents provide changes in the convective time delays that influence combustion instabilities while maintain a constant flame temperature (HSI).

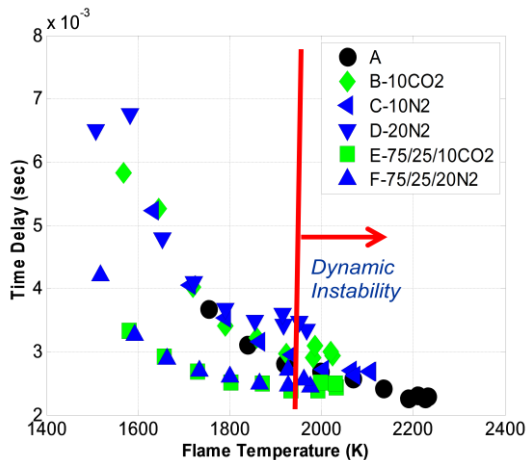


Figure 8b. The addition of fuel diluents provide changes in the convective time delays that influence combustion instabilities while maintain a constant flame temperature (LSI).

distribution.

changing the dynamic response (Figure 8a). This opens the possibility of utilizes a system with variable EGR to control the occurrence of thermoacoustic instabilities. Figure 8b shows a slightly different response from the LSI that is much less sensitive to changes in fuel composition.

V. Conclusions

Exhaust gas recirculation is a viable technology that could make post-combustion carbon capture system more economical for existing natural gas fire power plants. However changes in fuel composition as a result of EGR could alter the occurrence or severity of thermoacoustic instabilities. Changes in fuel composition, through the addition of diluents such as CO₂ and N₂ can alter the flame location thus changing the phasing of the originating disturbance and subsequent heat release.

Results from this study supported earlier findings that stressed the importance of convective time delays in unstable systems. Under high swirl combustion the amplitudes of the dynamic instabilities were reduced with the addition of a diluent in both methane and methane hydrogen fueled burners, even while maintaining a constant flame temperature. However, comparable dilution with N₂ and CO₂ resulted in a difference in the dynamic response as a result of variation in the convective time delay. Fuel substitution with 25% hydrogen and 10% CO₂ did produce similar results as the 10% N₂ dilution with methane. These results suggest that while the addition of diluent may reduce (or more precisely, “change”) the dynamic response, varying the amount of CO₂ through exhaust gas recirculation could have a larger effect than dilution with air or nitrogen. This opens the possibility of pursuing variable EGR as a means of controlling the dynamic response.

With low swirl combustion the flame exhibited the same basic behavior, as the dynamic response was linked to the convective time delay. However, the low-swirl flame appeared to be much less sensitive to changes in fuel composition suggesting the addition of diluents did not significantly alter the flame center of mass or heat release

Acknowledgments

The support of the U.S. DOE Turbines program is gratefully acknowledged. J. Ranalli gratefully acknowledges the support of the Oak Ridge Institute for Science and Education (ORISE) Postdoctoral Fellowship program.

References

1. Botero, C., Finkenrath, M., Bartlett, M., Chu, R., Choi, G., Chinn, D., “Redesign, Optimization and Economic Evaluation of a Natural Gas Combined Cycle with the Best Integrated Technology CO₂ Capture”, Energy Procedia, 2009, 1, pp3835-3842.
2. Klara, J., “The Potential of Advanced Technologies to Reduce Carbon Capture Costs in Future IGCC Power Plants”, Energy Procedia, 2009, 1, pp 3827-3834.

3. Griffin, T., Bücker, D., Pfeffer, A., "Technology Options for Gas Turbine Power Generation with Reduced CO₂ Emission", *J. Eng. Gas Turbines Power*, July 2008, 130.
4. El Kady, A., Evulet, A., Brand, A., Ursin, T.P., Lyngghjem, A., "Exhaust Gas Recirculation in DLN F-Class Gas Turbines for Post-Combustion CO₂ Capture", *ASME Turbo Expo 2008*, GT2008-51152, Berlin, Germany.
5. Rokke, P.E., Hustad, J.E., "Exhaust Gas Recirculation in Gas Turbines for Reduction of CO₂ Emissions", *Intl. J. Thermodynamics*, Sept 2005, 8, No. 4, pp 167-173.
6. Li, H., ElKady, A.M., Evulet, A.T., "Effect of Exhaust Gas Recirculation on NO_x Formation in Premixed Combustion System", *47th AIAA Aerospace Sciences*, January 2009, Orlando, Florida.
7. Lieuwen, T., Zinn, B., "Theoretical Investigation of Combustion Instability Mechanisms in Lean Premixed Gas Turbines", *AIAA 98-0641*, 36th AIAA Aerospace Sciences Meeting, January 1998, Reno, Nevada.
8. Lieuwen, T., McDonnell, V., Petersen, E., Santavicca, D., "Fuel Flexibility Influences on Premixed Combustor Blowout, Flashback, Autoignition and Stability", *ASME Turbo Expo 2006*, GT2006-90770, Barcelona, Spain.
9. Janus, M., Richards, G., Yip, J., "Effects of Ambient Conditions and Fuel Composition on Combustion Stability", 1997, *ASME 97-GT-266*.
10. Wicksall, D.M., Agrawal, A.K., "Acoustics Measurements in a Lean Premixed Combustor Operated on Hydrogen / Hydrocarbon Fuel Mixtures", *Intl. J. Hydrogen Energy*, 2007, 32, pp1103-1112.
11. Hendricks, A.G., Vandsburger, U., "The Effect of Fuel Composition on Flame Dynamics", *Experimental Thermal and Fluid Science*, October 2007, 32, No 1, Pages 126-132.
12. Richards, G., Straub, D.L., Robey, E.H., "Passive Control of Combustion Dynamics in Stationary Gas Turbines", *J Prop. Power*, Sept 2003, 19, No5.
13. Nord, L., Andersen, H.G., "Influence of Variations in the Natural Gas Properties on the Combustion Process in Terms of Emissions and Pulsations for a Heavy-Duty Gas Turbine", June 2003, *IJPGC2003-40188*, Atlanta, Georgia.
14. Tuncer, O., Acharya, S., and Uhm, J.H., "Dynamics, NO_x and flashback characteristics of confined premixed hydrogen-enriched methane flames," *International Journal of Hydrogen Energy* 34, no. 1 (January 2009): 496-506.
15. Cong, T.L., Dagaut, P., "Experimental and Detailed Kinetic Modeling of the Oxidation of Methane and Methane / Syngas Mixtures and Effect of Carbon Dioxide Addition", *Combust. Sci and Tech.*, 2008, 180, pp2046-2091.
16. Liu, F., Guo, H. and Smallwood, G., "The Chemical Effect of CO₂ Replacement of N₂ in air on the Burning Velocity of CH₄ and H₂ Premixed Flames", *Combustion and Flame* 2003, 133, 495-497.
17. Lohrmann, M.; Buchner, H. Prediction of stability limits for LP and LPP gas turbine combustors. *Combustion Science and Technology* 2005, 177, 2243-2273.
18. Palies, P.; Durox, D.; Schuller, T.; Candel, S. The combined dynamics of swirler and turbulent premixed swirling flames. *Combustion and Flame* 2010, 157, 1698-1717.
19. Johnson, M.; Littlejohn, D.; Nazeer, W.; Smith, K.; Cheng, R. A comparison of the flowfields and emissions of high-swirl injectors and low-swirl injectors for lean premixed gas turbines. *Proceedings of the Combustion Institute* 2005, 30, 2867-2874.
20. Kim, K.; Lee, J.; Quay, B.; Santavicca, D. Spatially distributed flame transfer functions for predicting combustion dynamics in lean premixed gas turbine combustors. *Combustion and Flame* 2010, 157, 1718-1730.
21. Cheng, R., and Littlejohn, D., Laboratory Study of pRemixed H₂-Air and H₂-N₂-Air Flames in a Low-Swirl Injector for Ultra-Low Emissions Gas Turbines, *Proceedings of the ASME Turbo Expo*; Montreal, Canada, 2007; GT2007-27512.
22. Kang, D.; Culick, F.; Ratner, A. Combustion dynamics of a low-swirl combustor. *Combustion and Flame* 2007, 151, 412-425.
23. (14) Yilmaz, I.; Ratner, A.; Ilbas, M.; Huang, Y. Experimental investigation of thermoacoustic coupling using blended hydrogen-methane fuels in a low swirl burner. *International Journal of Hydrogen Energy* 2010, 35, 329-336.
24. Ferguson, D.; Ranalli, J.; Strakey, P. In *Proceedings of the ASME Turbo Expo*; Glasgow, UK, 2010; Vol. GT2010-23642.
25. Lee, J.; Santavicca, D. Experimental diagnostics for the study of combustion instabilities in lean premixed combustors. *Journal of Propulsion and Power* 2003, 19, 735-750.